Scientific Papers Series Management, Economic Engineering in Agriculture and Rural Development
Vol. 22, Issue 4, 2022
PRINT ISSN 2284-7995, E-ISSN 2285-3952

USING RUBBER TUBES TO GENERATE MICRO BUBBLES FOR AERATION SYSTEM IN SEMI-INTENSIVE FISH FARMING

Tarek FOUDA[1], Abd-Elrahman ELRAYES[2], Abd-Elhameed ELHANAFY[2], Mohamed GHONAME[1]

[1]Tanta University, Faculty of Agriculture, Agriculture Engineering Department, Egypt, Emails: tfouda628@gmail.com., mohamed.ghonaim@agr.tanta.edu.eg
[2]Agriculture Research Center, Agricultural Engineering Research Institute, Egypt, Email: abdelhameedhamada111@gmail.com.

Corresponding author: tfouda628@gmail.com, tfouda@yahoo.com

Abstract

The expansion of aquaculture ponds necessitates the development of aeration and the addition of oxygen. Rubber tubes are a new way of aerating by generating micro bubbles on the water surface. Experiments were conducted to investigate and determine the effects of air flow rate, tube wall thickness, depth from the surface and design shape on saturation time, the oxygen mass transfer coefficient and standard aeration efficiency. To identify each indicator, testing were carried out in accordance with ASCE 2007 guidelines from the American Society of Civil Engineers. The findings demonstrated a connection between oxygen mass transfer coefficient and operational parameters were as follows: inverse relationship with air flow rate, inverse relationship with depth from water surface, positive relationship with tube wall thickness and increases with circular shape design more than longitudinal. The maximum value of standard aeration efficiency was 2.66 kg.O_2/kW.h under operational parameters of 0.1 $m^3.h^{-1}$ for air flow rate, 0.70 m for depth from the water surface, 7 mm for tube wall thickness and circular design shape. The minimum value of saturation time was 8 minutes under operational parameters of 0.1 $m^3.h^{-1}$ for air flow rate, 0.70 m for depth from the water surface, 7 mm for tube wall thickness and circular design shape.

Key words**:** *aquaculture, water quality, dissolved oxygen, aeration diffusion by fine bubbles*

INTRODUCTION

The quantity of fish produced increased by 5.4% to 2.0 million tonnes in 2019 from 1.90 million tonnes in 2018, mainly because more fish and rice fields were produced on farms. Lakes came in second with a production percentage of 79.7%, followed by marine waters with 4.9%, fresh water with 3.8%, and rice fields with 0.8% of the total amount of fish produced [5].

Egypt uses a variety of aquaculture techniques, such as circular tanks, dug earthen ponds, pens and enclosures, concrete and raceway ponds, and floating fish cages, among others. Additionally, semi-intensive clay pond aquaculture is the most common aquaculture practice in Egypt. Based on agricultural drainage waters, intense aquaculture farming has increased during the past 15 years, particularly in the deserts of northern Sinai [11].

Brackish water produced 855,789 t of tilapia in 2017, accounting for 70% of all tilapia produced in Africa. Egypt dominates the production of farmed tilapia in Africa. In 2017, the total amount of farmed tilapia produced in Africa was 79% (967,301 t), with Egypt producing the majority of that amount. Africa's contribution to the world's tilapia output will drop from 21% in 2017 to only 4.3% if Egypt's share is discounted. In Egypt, brackish water settings in the northern lakes regions along the Mediterranean coast are mostly used for tilapia culture. Egypt produced 854,808 t of tilapia from brackish water sources in 2017, accounting for 88.4% of the nation's overall (and 70% of the continent's) tilapia production [7].

Farmers must monitor water quality in order to spot trends in concentration changes and modify their management strategies accordingly. Numerous characteristics of water are connected and interact with one another, and changes in one variable might provide light on changes in another related one [20].

Due to the small amount of gill surface area that can absorb oxygen, the rate at which oxygen can be taken up is constrained, and sub-optimal DO concentrations slow down fish growth rates, the concentrations of DO in water are crucial. Also, mentioned that male Nile tilapia of the two size classes-large fish (>200 g) and little fish (100 g)-were studied to determine the effects of DO on feed intake and nitrogen and energy balances. On the other hand, larger fish had higher feed consumption when DO rose from 2.6 to 6.0 mg. L^{-1}, and the initial DO for these fish was around 5.5 mg. L^{-1}. As DO decreased, the fish tended to need less energy for upkeep. Gross energy consumption values, edible energy intake and metabolized energy intake were significantly increased for large fish as DO levels rose from 1.6 to 6.1 mg.L^{-1} [18].

More oxygen may dissolve in water when the temperature is lower. The application noted that water at a temperature of 32°C can contain up to 7.3 mg/l of oxygen, whereas water at a temperature of 7°C can hold 12.1 mg/l. Low oxygen levels will result from rising water temperatures. The dissolved oxygen levels at a given site are often larger in the winter than they are in the summer for this cause [13].

Dissolved oxygen is the amount of free, non-compound oxygen that is present in water or other liquids. It is a significant aspect in determining the water quality because of its effect on the aquatic life present in a body of water. After water, dissolved oxygen is the most crucial element in limnology which means the study of lakes. Aquatic life can be harmed and the quality of the water can be altered by too much or too little dissolved oxygen [12].

The minimum dissolved oxygen ranges for Oreochromis niloticus were 0.1-0.5 mg/l, while the best value was between 6 and 6.5 mg/l [1].

The most crucial period to introduce more aeration is shortly before dawn, when DO concentrations are often lowest because this is when they frequently drop below tolerable levels. Early morning DO for warmwater fish should stay above 3–4 mg/L, and above 5–6 mg/L for coldwater fish. Warmwater and coldwater fish, respectively, can survive with concentrations as low as 1.0-1.5 mg/L and 2.5-3.5 mg/L. However, these concentrations can raise stress, reduce appetite or aggression to eat, and - if low enough for a long length of time - they can be deadly [4].

Due to the local fish's higher metabolic rates while they are feeding, DO drops during feeding. Fish spend more energy to eat in a competitive manner, which causes an increase in metabolic rate. A DO requirement is also produced by uneaten feed and feces. This excrement provides plant nutrients that encourage the growth of phytoplankton. When phytoplankton is more abundant, the amount of DO that they need to breathe at night can increase. To raise the need for DO, phytoplankton are also continuously perishing and decomposing. The use of fertilizer can encourage the growth of algae, which can improve oxygen production and remove potentially hazardous ammonia [21].

The performance of tilapia may be significantly impacted by the interplay between diet mix and DO concentration. These researchers fed Nile tilapia (35 g) two different diets at two different oxygen saturation levels: normoxia (100%, 6.9 mg.L^{-1}) and hypoxia (50%, 3.5 mg.L^{-1}). The control diet was based on fishmeal (FM), while the other diet was based on soybean meal (SBM). Under normoxia, the FM "control" diet resulted in the highest growth rates [19].

The daily rate of partial water exchange in clay ponds is relatively low. In fact, early in the season, when the number of fish is minimal and well below the pond's carrying capacity, it might not even be necessary. However, as fish get bigger and bigger, there is a greater need for freshwater. Based on the stocking density, fish size, and species, it may reach 20% or more every day by the end of the season [14].

In the aquatic environment, direct diffusion from the air, wind wave action, and photosynthesis by aquatic plants are the three main sources of oxygen. When the water quality is good, oxygen molecules easily infiltrate the water until the oxygen volume is balanced. If the atmosphere's dissolved oxygen concentration is higher than

concentration in the water, which tends to diffuse in the air, the same thing could occur, but in the other direction [9].

The three essential parts of a diffused aeration system are an air pump, a diffuser, and connective tubing. Diffusers offer a variety of forms, including those with coarse, medium, and fine pore sizes. According to estimates, coarse, medium, and fine pore diffusers all function between 0.60 and 1.20 kg O_2/kW/hr, 1.0 to 1.6 kg O_2/kW/hr, and 1.2 to 2.0 kg O_2/kW/hr, respectively. Larger bubbles are produced by coarse pore diffusers, while smaller bubbles are produced by fine pore diffusers. Fouling and scaling, which are biological and chemical processes that damage diffuser functioning, can occur in diffusers. This necessitates periodic hydrochloric acid cleaning of diffusers [15].

The main aims of the research were:

-Evaluating fine bubbles tube aeration performance.

-Selecting the optimum operational conditions.

MATERIALS AND METHODS

Experimental setup

The experiment was established in an aquaculture private pond at Kafrelshikh government, Egypt. As indicated at figure 1, 2, 3 and table 1 stainless-steel tank with dimensions of 1×1×1 (m) for length, width and height, respectively used as water reservoir. The tank was filled up with 1 m^3 of tap water. An electric single phase compressor model APT (SGBM9037) of 1.5 hp, 25 L capacity, maximum pressure of 8 bar and maximum free air delivery:130 $L.min^{-1}$ used as a source of air injection. Three models of diffusion tubes D25-4, D25-6 and D25-7 which made from rubber and 1 m length for airmmax company, China with specification indicated in Table 1. Portable Galvanic Dissolved Oxygen Meter model HI9147 for HANNA company, USA used for estimation dissolved oxygen, water temperature and water salinity. Digital LCD anemometer and thermometer for measuring air wind speed and temperature. Digital vernier calliper of model SM-453, Japan used for estimating dimensions and diameters of experimental parts. Watt meter to estimate consumed energy in kW.h.

Experimental procedure

Main experiment established to evaluate rubber tube bubbles aeration method. Performance indicators estimated were: (1) Saturation time (2) K_La_{20} (3) SAE. According to (ASCE, 2007) tap water used in the experiment and changed after treatment. Deoxygenation of water attempted by adding 0.1 $mg.L^{-1}$ cobalt chloride ($CoCl.6H_20$) and 10-12 $mg.L^{-1}$ sodium sulfite ($NaSO_3$) for every $mg.L^{-1}$ of dissolved oxygen. Dissolved oxygen probe preferred to be at middle of the tank, and at least 20 cm from tank sides, surface and aeration equipment. Measuring process starts at the point of DO reads increase from zero concentrations and previous time neglected. Readings are recorded till reaching 80-85% of dissolved oxygen saturation concentration.

Theoretical considerations

The dissolved oxygen (C_e) concentrations at saturation are estimated using the following equation [17]:

$$C_e = \frac{125.9}{(32+1.8\,T)^{0.625}} \qquad eq\ (\mathbf{III.1})\ldots\ldots(1)$$

where:

C_e = Saturation concentration of oxygen, mg/L at atmospheric pressure;

T = Water temperature, °C.

When a force is created, mass transfer by diffusion happens between the two points. The relative pressure gradient drives the gas phase, whereas the concentration gradient drives the water phase. The formula for oxygen transfer [8] is as follows:

$$\frac{dm}{dt} = -D_l \times A\frac{dc}{dy} \qquad eq\ (\mathbf{III.2})\ldots\ldots(2)$$

where:

$\frac{dm}{dt}$ is the proportion of diffusion mass transfer,

DL is the oxygen molecular diffusion in water coefficient,

A is the diffusion cross sectional area and expressed as m^2/s, and $\frac{dc}{dy}$ is the oxygen concentration gradient perpendicular to the cross-sectional area and mentioned by $kg/m^3/m$.
So, the above equation could mention as:

$$\frac{dm}{dt} = -D_g \times A\left[\frac{dc}{dy}\right]_g = -D_l \times A\left[\frac{dc}{dy}\right]_l = -D_e \times A\left[\frac{dc}{dy}\right]_e \quad eq\ (\mathbf{III.3})..(3)$$

where:

where, $\left[\frac{dc}{dy}\right]_g$ is the concentration inclination in gas layer, $\left[\frac{dc}{dy}\right]_l$ is the concentration gradient in Water layer, $\left[\frac{dc}{dy}\right]_e$ is the concentration inclination in the body of the Water, D_g is the coefficient molecular diffusion of oxygen in gas medium and D_e is the eddy diffusion coefficient of the oxygen in the medium of the Water.

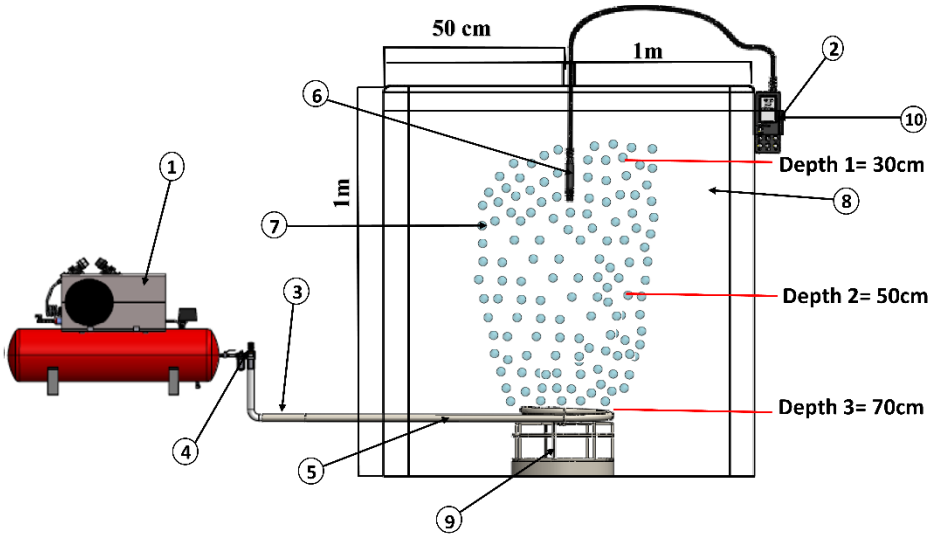

NO	ITEM
1	Air Compressor
2	Dissolved Oxygen Meter
3	Air Compressor Tube
4	Air flow valve
5	Tube
6	Sensor
7	Bubbles
8	Tap Water
9	Tube Holder
10	Dissolved Oxygen Meter Holder

Fig. 1. Schematic diagram of the experiment.
Authors' drawing.

Table 1. Specification of different tubes models under study

Item \ Model	Unit	D25-4	D25-6	D25-7
Outer diameter (OD)	mm	25	25	25
Inner diameter (ID)	mm	16	13	11
Wall thickness (Wall)	mm	4	6	7

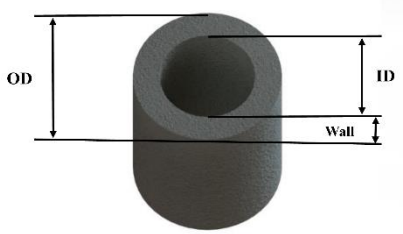

Fig. 2. Schematic diagram of rubber tube and its parts.
Source: Authors' drawing.

a) Longitudinal shape

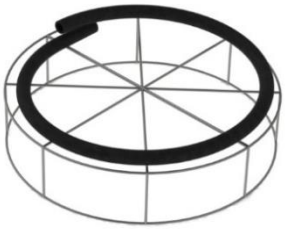

b) Circular shape

Fig. 3. Design shapes of diffusion tubes.
Source: Authors' drawing.

This Equation might be as:

$$\frac{dm}{dt} = \frac{D_L}{y_L} A \times \Delta C = K_L = A \times \Delta C \quad eq\ (\mathbf{III.4})...(4)$$

where:
Y_L is the thickness of Water layer,
ΔC is shortage of oxygen = C* − C, C* is equivalent concentration at the surface, and C is the concentration in the water state. $K_L = \frac{D_L}{y_L}$ and K_L is identified as the water layer coefficient. Previous equation can be stated in concentration by volume, V, of the water:

$$\frac{1}{V} \times \frac{dm}{dt} = \frac{dc}{dy} = K_L \times \frac{A}{V} \times \Delta C \qquad eq\ (\mathbf{III.5}).....(5).$$

In non-natural aeration methods, it is very difficult to estimate the interfacial area because of the turbulent surface. Hence $K_L \frac{A}{V}$ is substituted by coefficient transfer K_{La} of the method, and its units is h^{-1}. Therefore, previous equation shows K_{La} as:

$$\frac{dc}{dt} = K_L \times a_T \times \Delta Cz = K_L \times a_T \times (C^* - C) \qquad eq\ (\mathbf{III.6})....(6)$$

Accumulation of K_L and a_T, $K_L a_T$ a generated expression is used as the overall coefficient of oxygen transfer. By integrating previous equation for C among C_0 and C_t and t = 0 to t, the following terminologies are obtained.

$$\ln \frac{C^* - C_t}{C^* - C_0} = K_L \times a_T \times (t - t_0) \qquad eq\ (\mathbf{III.7})....(7)$$

$$C_t = C^* - (C^* - C_0) exp[-K_L \times a_T \times (t - t_0)] \qquad eq\ (\mathbf{III.8})..(8)$$

where:
$K_L a_T$ is the coefficient of overall oxygen transfer (h^{-1}),
C_0 is the start concentration of oxygen in sample (mg/L),
C_t is the water concentration of oxygen in end at time t (mg/L) and
($C^* - C_0$) is the oxygen loss (mg/L).
According to the ASCE Method, the coefficient of overall oxygen transfer ($K_L a_T$) of previous equation can be estimated by the Nonlinear Regression Method. Previous equation was used to calculate the three variables, C*, C_0, and $K_L a_T$ [16].
At standard conditions of temperature (20°C), $K_L a_t$ was calculated:

$$K_L \times a_{20} = \frac{K_L \times a_T}{\theta^{(T-20)}} \qquad eq\ (\mathbf{III.9})...(9)$$

where:
θ means correction factor of temperature (θ = 1.024 for tap water) [6].
By using dissolved oxygen drop the oxygen transfer rate (OTR) of aeration device is definite as the quantity of oxygen mass that the tool added into water at specified time [2].

$$OTR = K_L a_T \times \Delta C \times V \qquad eq\ (\mathbf{III.10})....(10)$$

where:
ΔC, the difference between C* and C_0, V is the quantity of water in trial tank (m^3), for typical conditions at 20°C the rate of oxygen transfer (OTR) mentioned as:

$$OTR = K_L a_{20} \times \Delta C \times V \qquad eq\ (\mathbf{III.11})....(11).$$

In case of evaluation under standard conditions of water temperature = 20°C, start DO = 0 mg/L, atmospheric pressure = 1atm and pure tap water) $/h^{-1}$ [2], hence this terminology express the standard oxygen transfer rate (SOTR) as follow:

$$SOTR = (K_L a)_{20} \times \Delta C \times V \qquad eq\ (\mathbf{III.12})....(12).$$

The standard oxygen transfer rate (SOTR), which is used to compare various aeration equipment, is used to determine which is better. The formula for the actual oxygen transfer rate (OTR_f) is given as follow [3]:

$$OTR_f = \frac{SOTR[\propto \times \theta^{T-20}(\beta C_s - C_p)]}{9.07} \qquad eq\ (\mathbf{III.13}).....(13).$$

The quantity of oxygen transmitted (kg) per requested power, or standard aeration efficiency, is the optimum metric for evaluating different oxygenation techniques. Use the following equation to determine SAE:

$$SAE = \frac{SOTR}{P} \qquad eq\ (\mathbf{III.14}).....(14)$$

where:
P is the required power by the aerator under operating conditions (kW).
Variables under study were: permissible limits for operational parameters at aquaculture earthen ponds were: (1) three air flow ranges (0.554, 0.969 and 1.246 $m^3.h^{-1}$), (2) three depths from water surface (0.3, 0.5 and 0.7 m), (3) three tube wall thickness (4, 6

and 7 mm), (4) two design shapes (longitudinal and circular) [10].

RESULTS AND DISSCUSIONS

Effect of aeration by fine bubbles on oxygen productivity

Effect of aeration by fine bubbles on saturation time

Figures show the effect of air flow rate, depth from the surface, thickness of tube wall and design shape on saturation time as shown in Figures 4, 5 and 6. Under operational conditions of 1.246 $m^3.h^{-1}$ air flow rate, 0.30 m depth from water surface, 4 mm tube wall thickness, and longitudinal design shape, the highest value of saturation time was 22 minutes.

The lowest value of saturation time was 8 minutes under operational parameters of 0.554 $m^3.h^{-1}$ for air flow rate, 0.70 m for depth from water surface, 7 mm for tube wall thickness and circular design shape.

a) The effect of air flow quantity on saturation time

The rise of air flow rate from 0.556 to 1.246 m^3. h^{-1} leaded to increase at saturation time with 66 % (from 12 to 20 minutes) at depth from water surface of 30 mm, tube wall thickness of 4 mm and circular design shape as shown in Figures 4, 5 and 6.

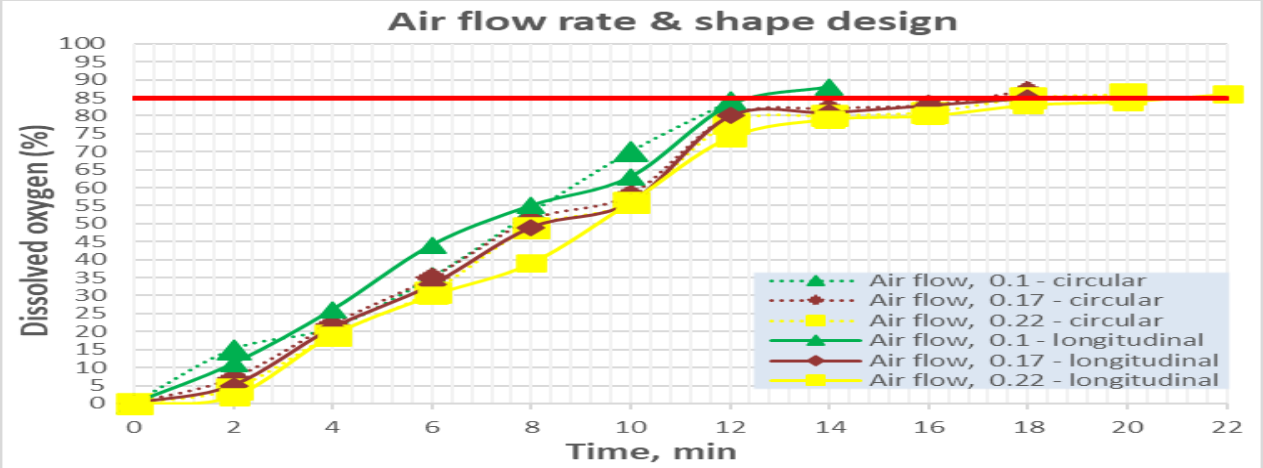

Fig. 4. The impact of air flow rate and shape design on saturation time at a wall thickness of 4 mm and a depth of 0.3 m. Source: Authors' determination.

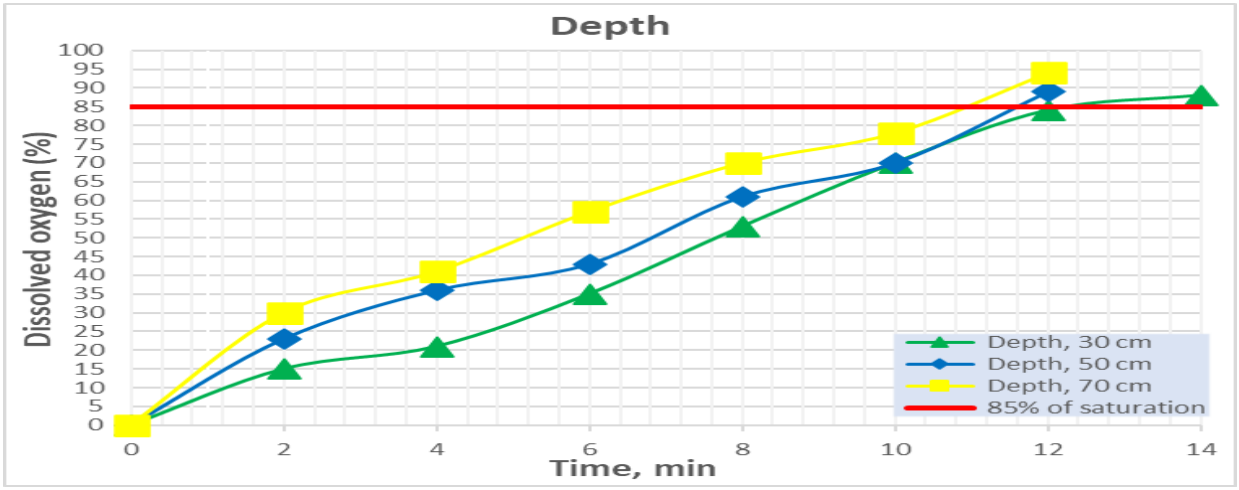

Fig. 5. Impact of diffusion tube submergence on saturation time for 0.554 $m^3.h^{-1}$ air flow rate and circular form design and 4 mm wall thickness
Source: Authors' determination.

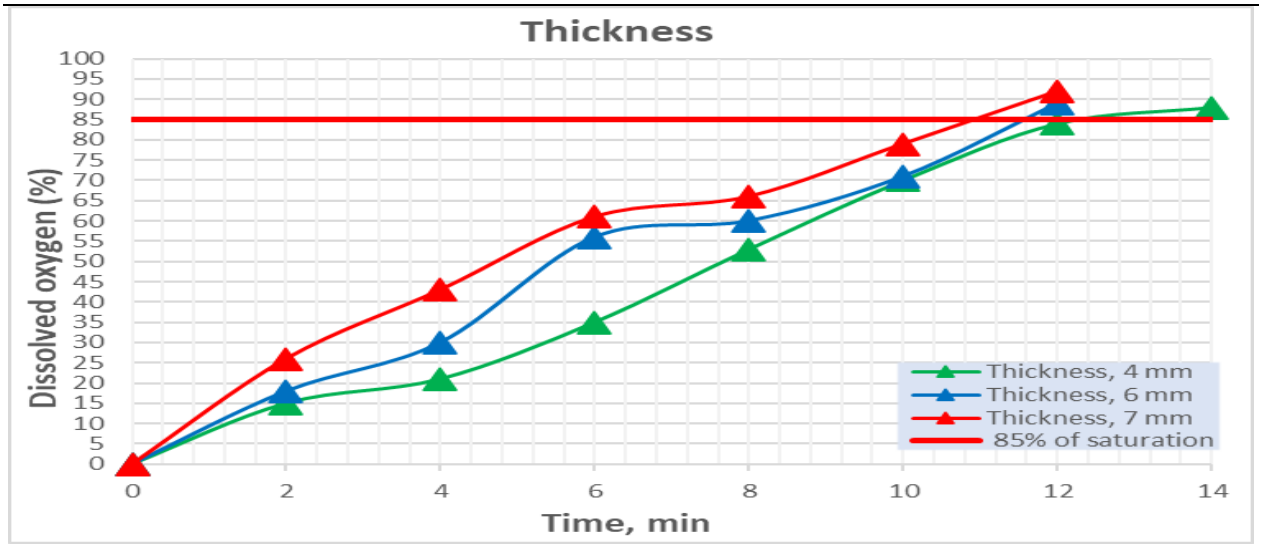

Fig. 6. Impact of diffusion tube wall width on saturation time for 0.554 $m^3.h^{-1}$ air flow quantity and circular form design and 0.3 m depth
Source: Authors' determination.

This might be described as an increase in air flow rate generated an rise in bubble size, which in turn instigated an rise in bubble velocity, resulting in less time spent in water and less overlap between air and water.

b) The effect of depth from water surface on saturation time

The increase of depth from water surface from 0.3 to 0.7 m resulted in decrease at saturation time with 15 % (from 13 to 11.5 minutes) at air flow rate from 0.556 $m^3.h^{-1}$, tube wall thickness of 4 mm and circular design shape as shown in figures 4, 5 and 6.

Increased interaction time between water and diffused air resulted in an increase in saturation time when depth from the water surface was increased.

c) The effect of tube wall thickness on saturation time

The increase of tube wall thickness from 4 to 7 mm resulted in decrease at saturation time with 15.3 % (from 13 to 10.5 minutes) at air flow rate from 0.556 $m^3.h^{-1}$, depth from water surface of 0.3 m and circular design shape as shown in figures 4, 5 and 6.

This could be because increasing the thickness resulted in a drop in pore widths, resulting in a reduction in the size of generated bubbles with a low velocity and longer interaction time.

d) The effect of shape design on saturation time

The changing of shape design from circular to longitudinal led to increase in saturation time with 3.8 % (from 13 to 13.5 minutes) at air flow rate from 0.556 $m^3.h^{-1}$, depth from water surface of 0.3 m and tube wall thickness of 4 mm as shown in Figures 4, 5 and 6.

When the shape was changed from circular to longitudinal, the projected area dispersed.

Effect of aeration by fine bubbles on oxygen mass transfer coefficient

Figures 7, 8 and 9 show the impact of air flow rate, deepness from the surface, thickness of tube wall and design form on the oxygen mass transfer coefficient.

The highest measure of oxygen mass transfer coefficient was 11.581 h^{-1} under operational parameters of 0.554 $m^3.h^{-1}$ for air flow rate, 0.70 m for depth from water surface, 7 mm for tube wall thickness and circular design shape as shown in Figures 7, 8 and 9.

The minimum value of oxygen mass transfer coefficient was 3.899 h^{-1} below operational conditions of 1.246 $m^3.h^{-1}$ for aeration flow rate, 0.30 m for deepness from water surface, 4 mm for tube wall thickness and longitudinal design form.

a) The impact of aeration flow rate on the oxygen mass transfer coefficient

The rise of air flow quantity from 0.554 to 1.246 $m^3.h^{-1}$ caused to lower oxygen mass transfer coefficient with 17.38 % (from 5.425 to 4.482 h^{-1}) at depth from water surface of 0.30 m, tube wall thickness of 4 mm and

circular design shape as shown in Figures 7, 8 and 9.

This result could be explained as increase in air flow rate led to increase in bubble size which caused increase in bubble velocity so, the time spent in water and overlap between air and water reduced. So, the relationship between oxygen mass transfer factor and air flow quantity was inverse relationship.

b) The impact of depth from water surface on the oxygen mass transfer coefficient

The increase of submergence from water surface from 0.3 to 0.7 m caused in rise at oxygen mass transfer coefficient with 53.53 % (from 5.425 to 8.329 h^{-1}) at air flow rate from 0.554 $m^3.h^{-1}$, tube wall thickness of 4 mm and circular design shape as shown in Figures 7, 8 and 9.

Increasing depth from water surface led to increase interaction time between water and diffused air so increase in oxygen mass transfer coefficient.

c) The impact of tube wall thickness on the oxygen mass transfer coefficient

The growing of tube wall thickness from 4 to 7 mm caused in rise at oxygen mass transfer coefficient with 37.82 % (from 5.425 to 7.477 h^{-1}) at air flow rate from 0.554 $m^3.h^{-1}$, depth from water surface of 0.3 m and circular design shape as shown in figures 7, 8 and 9.

This result may be due to increasing the thickness which led to decrease in pores diameters consequently decrease at size of produced bubbles which had low velocity and more interaction time.

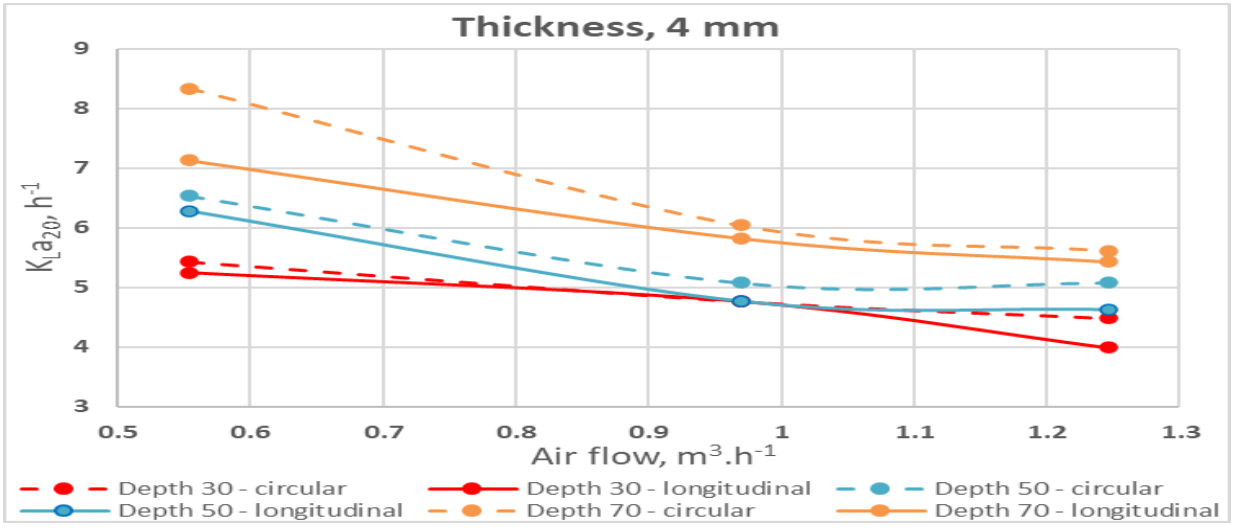

Fig. 7. Effect of air flow rate, depth and shape design on the oxygen mass transfer coefficient for 4 mm wall thickness

Source: Authors' determination.

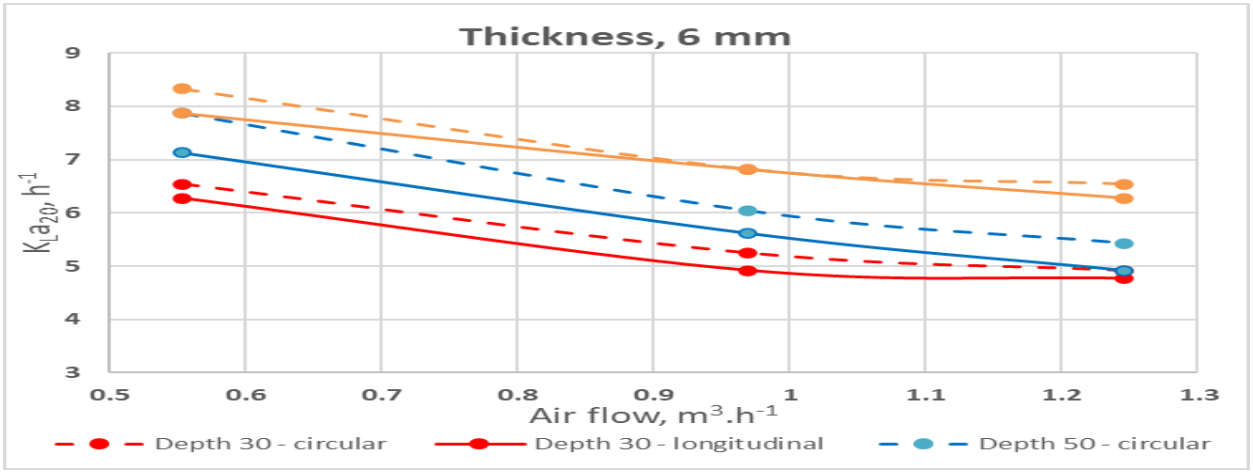

Fig. 8. impact of air flow quantity, submergence and form design on the oxygen mass transfer coefficient for 6 mm wall thickness

Source: Authors' determination.

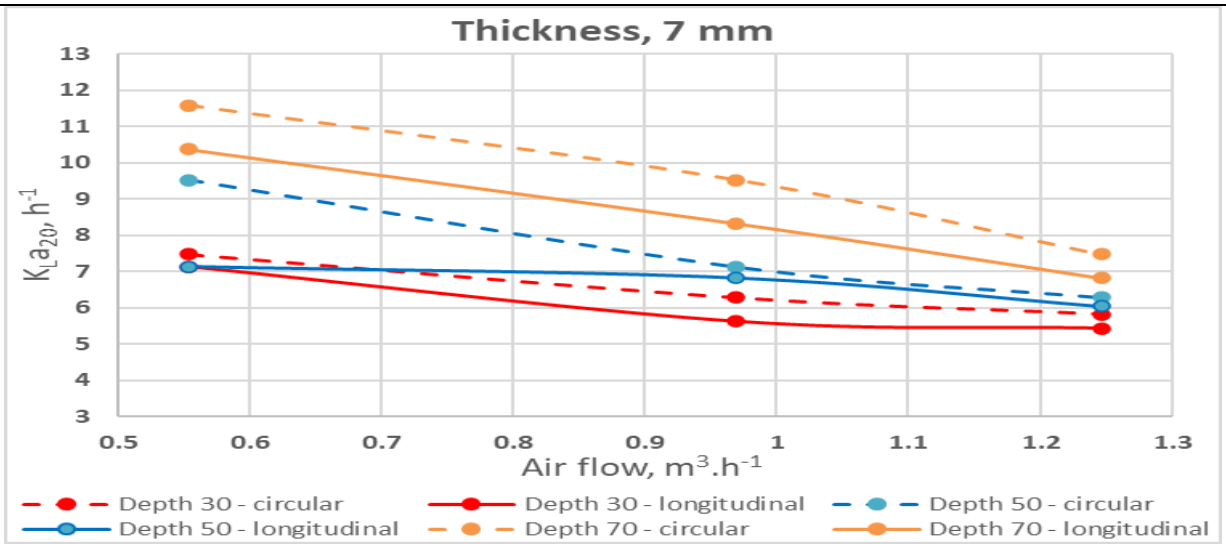

Fig. 9. impact of air flow quantity, submergence and form design on the oxygen mass transfer coefficient for 7 mm wall thickness
Source: Authors' determination.

d) The impact of form design on the oxygen mass transfer coefficient

The varying of form design from circular to longitudinal caused decrease of oxygen mass transfer coefficient with 3.3 % (from 5.425 to 5.246 h^{-1}) at air flow rate from 0.554 $m^3.h^{-1}$, depth from water surface of 0.3 m and tube wall thickness of 4 mm as shown in figures 7, 8 and 9. Changing shape design from circular to longitudinal led to dispersal in projected area.

Effect of aeration by fine bubbles tubes on standard aeration efficiency

Figure and table show the influence of air flow rate, depth from the surface, thickness of tube wall and design shape on standard aeration efficiency.

The maximum value of standard aeration efficiency was 2.66 kg.O_2/kW.h under operational parameters of 0.556 $m^3.h^{-1}$ for air flow rate, 0.70 m for depth from water surface, 7 mm for tube wall thickness and circular design shape as shown in Figures 10, 11 and 12.

The minimum value of standard aeration efficiency was kg.O_2/kW.h under operational parameters of 0.1.246 $m^3.h^{-1}$ for air flow rate, 0.30 m for depth from water surface, 4 mm for tube wall thickness and longitudinal design shape.

a) The impact of air flow rate on standard aeration efficiency

The rise of air flow rate from 0.554 to 0.1.246 $m^3.h^{-1}$ leaded to decrease at standard aeration efficiency with 67 % (from 1.246 to 0.411 kg.O_2/kW.h) at depth from water surface of 30 mm, tube wall thickness of 4 mm and circular design shape as shown in Figures 10, 11 and 12.

This result could be explained as increase in air flow rate led to increase in bubble size which caused increase in bubble velocity so, the time spent in water and overlap between air and water decreased. Hence the association between Standard aeration efficiency and aeration flow rate was inverse relationship.

b) The impact of submergence from water surface on standard aeration efficiency

The increase of depth from water surface from 0.3 to 0.7 m resulted in increase at standard aeration efficiency with 53.5 % (from 1.246 to 1.913 kg.O_2/kW.h) at air flow rate from 0.556 $m^3.h^{-1}$, tube wall thickness of 4 mm and circular design shape as shown in Figures 10, 11 and 12.

Increasing depth from water surface led to increase interaction time between water and diffused air so increase in Standard aeration efficiency.

c) The effect of tube wall thickness on standard aeration efficiency

The increase of tube wall thickness from 4 to 7 mm resulted in increase at standard aeration efficiency with 37.8 % (from 1.246 to 1.717 kg.O_2/kW.h) at air flow rate from 0.556 $m^3.h^{-1}$,

depth from water surface of 0.3 m and circular design shape as shown in figures 10, 11 and 12.

This result may be due to increasing the thickness which led to decrease in pores diameters consequently decrease at size of produced bubbles which had low velocity and more interaction time.

d) The effect of shape design on standard aeration efficiency

The changing of shape design from circular to longitudinal led to decrease of standard aeration efficiency with 3.4% (from 1.246 to 1.204 kg.O_2/kW.h) at air flow rate from 0.556 $m^3.h^{-1}$, depth from water surface of 0.3 m and tube wall thickness of 4 mm as shown in Figures 10, 11 and 12.

Changing shape design from circular to longitudinal led to dispersal in projected area.

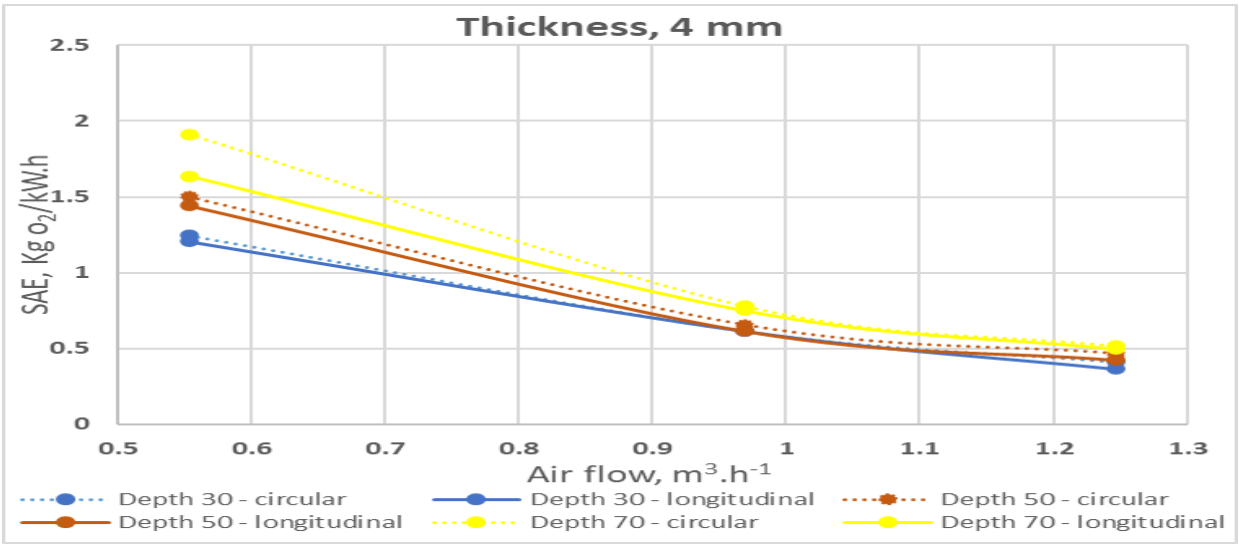

Fig. 10. Impact of air flow rate, submergence and form design on standard aeration efficiency for 4 mm wall thickness. Source: Authors' determination.

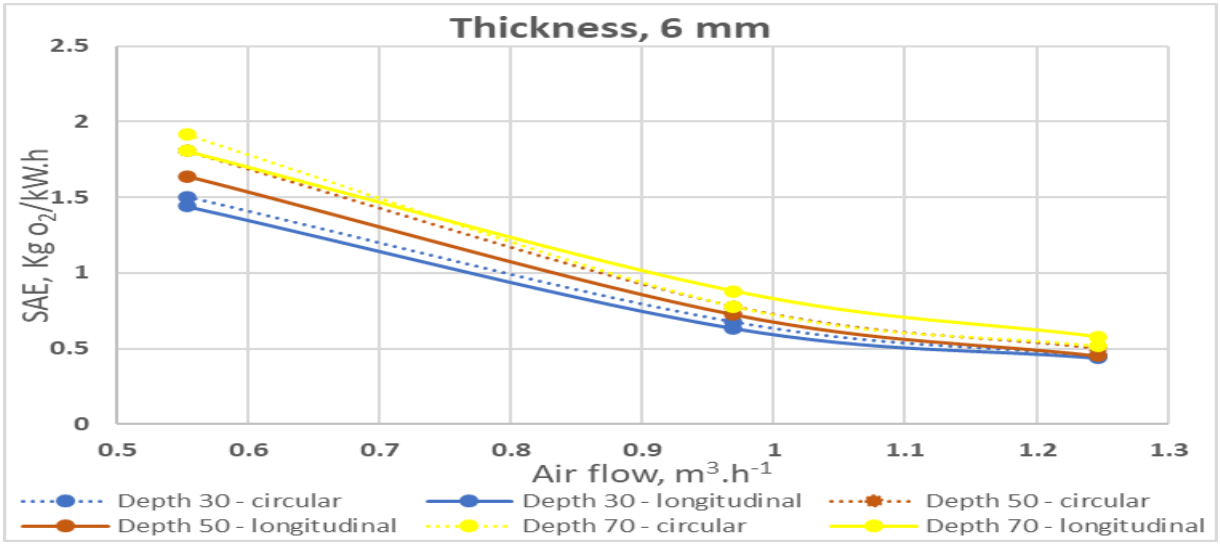

Fig. 11. Impact of aeration flow rate, submergence and form design on standard aeration efficiency for 6 mm wall thickness. Source: Authors' determination.

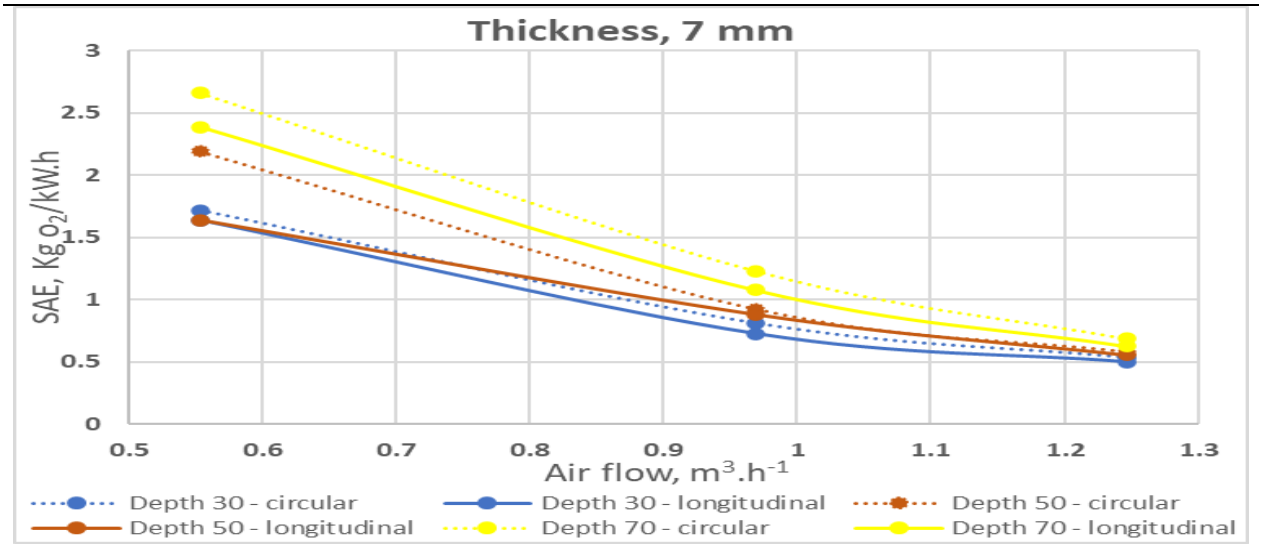

Fig. 12. Impact of aeration flow rate, submergence and form design on standard aeration efficiency for 7 mm wall thickness. Source: Authors' determination.

CONCLUSIONS

The experimental research found that:

-The relationship between oxygen mass transfer coefficient and operational parameters were as flow: inverse relationship with air flow rate, inverse relationship with depth from water surface, positive relationship with tube wall thickness and increases with circular shape design more than longitudinal.

-The relationship between standard aeration efficiency and operational parameters were as flow: inverse relationship with air flow rate, inverse

-Relationship with depth from water surface, positive relationship with tube wall thickness and increases with circular shape design more than longitudinal.

-As mentioned above the relationship between saturation time and operational parameters were as flow: positive relationship with air flow rate, positive relationship with depth from water surface, inverse relationship with tube wall thickness and increases with longitudinal shape design more than circular.

- The maximum value of standard aeration efficiency was 2.66 kg.O_2/kW.h under operational parameters of 0.554 $m^3.h^{-1}$ for air flow rate, 0.70 m for depth from the water surface, 7 mm for tube wall thickness and circular design shape.

- The minimum value of saturation time was 8 minutes under operational parameters of 0.554 $m^3.h^{-1}$ for air flow rate, 0.70 m for depth from the water surface, 7 mm for tube wall thickness and circular design shape.

REFERENCES

[1]Abdel-Tawwab, M., Hagras, A. E., Elbaghdady, H. A. M., Monier, M. N., 2014, Dissolved oxygen level and stocking density effects on growth, feed utilization, physiology, and innate immunity of Nile Tilapia, Oreochromis niloticus. Journal of Applied Aquaculture, 26(4), 340-355.

[2]ASCE, 2007, Measurement of oxygen transfer in clean water. American Society of Civil Engineers.

[3]Boyd, C. E., 1998, Pond water aeration systems. Aquacultural engineering, 18(1), 9-40.

[4]Boyd, C. E., 2015, Water quality, an introduction, 2nd edition. Springer, New York, New York, USA.

[5]CAPMAS, 2021, Central Agency for Public Mobilization and Statistics. Egypt

[6]Eckenfelder, Jr, W. W., Barnhart, E. L., 1961, The effect of organic substances on the transfer of oxygen from air bubbles in water. AIChE Journal, 7(4), 631-634.

[7]El-Sayed, A. F. M., 2019, Tilapia culture. Academic Press.

[8]Fick, A., 1855, On liquid diffusion. The London, Edinburgh, and Dublin Philosophical Magazine and Journal of Science, 10(63), 30-39.

[9]Floyd, R.F., 2011, Dissolved Oxygen for fish production, Fisheries and aquatic sciences department, Florida Cooperative Service, Institute of Food and Agricultural Sciences, University of Florida October 2011.

[10]Fouda, T., Elrayes, A, Elhanafy, A., 2022, A study on micro bubbles aeration method on water turbidity at aquaculture earthen ponds under different operational conditions. Scientific Papers Series Management, Economic Engineering and Rural Development, Vol. 22(3), 2022.

[11]Ghanem, A., Haggag, M., 2015, Assessment of the feasibility of using filter made of rice straw for treating aquaculture effluents in Egypt. Resources and Environment, 5(5), 135-145.
[12]Kemker, C., 2013, Dissolved Oxygen. Fundamentals of Environmental Measurements. Fondriest Environmental, Inc. 19.
[13]Murphy, S., 2012, General Information on Dissolved Oxygen. http://bcn.boulder.co.us /basin/data/BACT/info/DO.html http://bcn.boulder.co.us/basin/data/BACT/info/DO.html, Accessed on May, 2014.
[14]Nasr-Allah, A., Dickson, M., Al-Kenawy, D.A., Ibrahim, N., Ali, S.E., Charo-Karisa, H., 2021, Better management practices for tilapia culture in Egypt. Penang, Malaysia: CGIAR Research Program on Fish Agri-Food Systems. Manual: FISH-2021-03.
[15]Pentair, 2014, Aquatic Eco-Systems 2014 Master Catalog. 50-104.
[16]Rosso, D., Jiang, L. M., Hayden, D. M., Pitt, P., Hocking, C. S., Murthy, S., Stenstrom, M. K., 2012, Towards more accurate design and specification of aeration systems using on-site column testing. Water Science and Technology, 66(3), 627-634.
[17]Soderberg, R. W., 2020, Flowing water fish culture. CRC Press.
[18]Tran-Duy, A., Schrama, J. W., van Dam, A. A., Verreth, J. A., 2008, Impacts of dissolved oxygen levels and body weight on maximum feed intake, growth and hematological parameters of Nile tilapia, Oreochromis niloticus. Aquaculture, 275(1-4), 152-162.
[19]Tran-Ngoc, K.T., Dinh, N.T., Nguyen, T.H., Roem, A.J., Schrama, J.W., Verreth, J.A.J., 2016, Interaction for dissolved oxygen levels and diet composition on growth, digestibility and intestinal health of Nile tilapia (*Oreochromis niloticus*). Aquaculture 462, 101-108.
[20]Xu, Z., Xu, Y. J., 2016, A deterministic model for predicting hourly dissolved oxygen change: development and application to a shallow eutrophic lake. Water, 8 (2), 41.
[21]Zhou, L., Boyd, C. E., 2015, An assessment of total ammonia nitrogen concentration in Alabama (USA) ictalurid catfish ponds and the possible risk of ammonia toxicity. Aquaculture, 437, 263-269.